Preparation and Characterization of Polyethylene-*g*-Maleic Anhydride–Styrene/Montmorillonite Nanocomposites

Zhengfa Zhou,[1] Hongbo Zhai,[1] Weibing Xu,[1] Hanyang Guo,[1] Changfeng Liu,[1] Wei-Ping Pan[2]

[1]*Department of Polymer Science and Engineering, Hefei University of Technology, Hefei 23009, Anhui, People's Republic of China*
[2]*Department of Chemistry, Materials Characterization Center, Western Kentucky, Bowling Green, Kentucky 42101*

ABSTRACT: It is difficult to prepare polyethylene/montmorillonite by direct melt mixing because of the difference in character between polyethylene and montmorillonite. Therefore, it is necessary to modify polyethylene with polar groups, which can increase the hydrophilicity of polyethylene. At the same time, the inorganic montmorillonite should be modified with long-chain alkyl ammonium to increase the basing space between the interlayers. Thus, through the grafting of the polar monomer onto the main chain of polyethylene by reactive extrusion, polyethylene/montmorillonite nanocomposites can be prepared by the melt mixing of the grafter and organic montmorillonite. Fourier transform infrared has been used to prove that the monomers are grafted onto polyethylene. X-ray diffraction and transmission electron microscopy have been employed to characterize the nanocomposites. Furthermore, thermogravimetric analysis measurements show that the thermal stability of the nanocomposites is improved in comparison with that of the virgin materials. © 2006 Wiley Periodicals, Inc. J Appl Polym Sci 101: 805–809, 2006

Key words: graft copolymers; nanocomposites; polyethylene (PE)

INTRODUCTION

Polymer/clay nanocomposites are a class of hybrid materials composed of an organic polymer matrix in which inorganic particles with nanoscale dimensions are embodied.[1–4] At this scale, the inorganic fillers dramatically improve the properties of the polymer even with a small loading. The nanocomposites exhibit an improved modulus, lower thermal expansion coefficient and gas permeability, higher swelling resistance, and enhanced ionic conductivity in comparison with the pristine polymers, presumably because of the nanoscale structure of the hybrids and the synergism between the polymer and the silicate.[5,6] Since nylon 6/clay nanocomposites with excellent mechanical properties were developed by the Toyota group, much attention has been devoted to polymer/clay nanocomposites.[7–9]

The most commonly used clay is montmorillonite (MMT), which belongs to the general family of 2:1 layered silicates. Their structures consist of two fused silica tetrahedral sheets sandwiching an edge-shared octahedral sheet of either aluminum or magnesium hydroxide. The silicate layers are coupled through relatively weak dipolar and van der Waals forces. The Na^+ or Ca^{2+} residing in the interlayers can be replaced by organic cations such as alkylammonium ions via an ion-exchange reaction to render the hydrophilically layered silicate organophilic. In most cases, the synthesis of polymer/MMT nanocomposites has been reported via an intercalated polymerization process or melt-direct intercalation. Of the two ways, melt-direct intercalation is promising because this process does not need any solvent. Therefore, it is easily applied in industry.[10]

Polyethylene (PE) is one of the most widely used polyolefin polymers. Because it does not include any polar group in its backbone, it has not been thought that a homogeneous dispersion of clay layers in PE can be realized. Alexandre et al.[11] reported the preparation of PE/layered silicate nanocomposites by the polymerization-filling technique. Shin et al.[12] used bifunctional organic modifiers to prepare PE/clay hybrid nanocomposites by in situ polymerization. Zhang and Wilkie[13] acquired low-density PE/clay nanocomposites with good flammability properties via melt mixing in a Brabrender mixer. The results reported for polypropylene/clay hybrid preparation show that the chemical modification of these resins, particularly the grafting of pendant anhydride groups, is a useful way to overcome problems associated with poor phase adhesion in polyolefin/clay systems.[10,14,15] Therefore,

Wang and coworkers[16–18] prepared linear low-density PE/clay nanocomposites by grafting the polar monomer MAH to the backbone. Gopakumar et al.[19] also obtained PE/clay nanocomposites by direct-melt intercalation and investigated its nonisothermal crystallization kinetics.

PE will crosslink when a peroxide, such as dicumyl peroxide (DCP), is used to initiate the graft reaction by reactive extrusion. In general, an electron-donating molecule should be added to the reaction system to restrain the crosslinking reaction. In this study, we tried to use styrene (St) as a cograft monomer to stabilize the active radical to control the crosslinking reaction; this has been proved to be a useful way to control the decomposition reaction happening in the grafting process of polypropylene. At the same time, during the preparation of MAH-grafted high-density polyethylene (HDPE), the MAH monomer attached to the main chains just as a monomolecule because it was almost impossible for MAH to polymerize itself. However, when St was added, it could increase the length of the side chain because it was easy for the anhydride and St to copolymerize; this beneficial for improving the compatibility between the matrix and filler. Thus, in this study, a new kind of grafter, maleic anhydride–styrene cografted polyethylene (PE-g-MAH–St), was prepared by reactive extrusion. By the melt mixing of the grafter and organic MMT, PE/MMT nanocomposites were successfully obtained; this was proved by X-ray diffraction (XRD) and transmission electron microscopy (TEM). At the same time, the thermal and crystallization properties of the nanocomposites were also investigated via thermogravimetric analysis (TGA) and differential scanning calorimetry (DSC), respectively.

EXPERIMENTAL

Materials

HDPE was purchased from Dushanzi Chemical Co. (Xingjiang, China), Na$^+$ MMT was acquired from Zhejiang Fenghong Clay Chemical Co., Ltd. (Dinjan, China), and organic MMT was synthesized in our own laboratory according to ref. 9. MAH, DCP, and St were obtained from Shanghai Chemical Reagent Co., Ltd. (Shanghai, China).

Preparation of the grafter by reactive extrusion

HDPE and MAH (3 wt %) were premixed in the mixer at first. Then, DCP and St were added during the mixing process. After mixing for 5 min, the mixture was extruded in a single-screw extruder with a constant speed of 30 rpm. The grafter was called PE-g-MAH–St. The ratio of MAH to St was set to 1.

Preparation of the PE-g-MAH–St/MMT nanocomposites

First, PE–MAH–St and organic MMT were melt-mixed on two rollers for 10 min at 175°C. The mixture was press-molded to get a plate 4 mm thick. The concentration of organic MMT was set to 1, 3, or 5 wt %, and the acquired materials were defined as PMST1, PMST3, and PMST5, respectively.

Measurements

IR analysis of the grafter

After the grafter was dried for 8 h, 2 g of the grafter was weighed and put in a flask with 100 mL of xylene; the flask was then heated. After the grafter was completely dissolved in xylene, the solution was poured into 250 mL of acetone. The precipitate was filtered and dried at 60°C for 24 h. The dried precipitate was pressed into a film 0.1 mm thick and characterized with a WQF 300 Fourier transform infrared (FTIR) instrument.

Graft efficiency (DG) of PE-g-MAH–St

The filtered and dried precipitate (0.2–0.4 g) was put in a flask with 50 mL of xylene and completely dissolved. Then, the cooling solution was poured into 20 mL of ethanol/potassium hydroxide, and the solution was heated and refluxed. After 4 h, the chemical titration of this solution was carried out with a muriatic acid/ethanol solution. Therefore, DG of MAH can be calculated according to the following formula:

$$DG\ (\%) = [(V_1 - V_2)NM/1000\,W] \times 100\% \quad (1)$$

where V_1 is the volume of muriatic acid in the base experiment, V_2 is the volume of muriatic acid of the grafter PE-g-MAH–St, N is the concentration of muriatic acid, M is the molecular weight of MAH, and W is the weight of the precipitate. DG of PE-g-MAH–St prepared in this study was about 0.7 wt %.

Analysis of XRD

XRD was carried out with a Rigaku X-ray generator (Cu Kα radiation with $\lambda = 1.5406$ Å) (Tokyo, Japan) at room temperature. The diffractograms were scanned in the 2θ range of 1.2–10° at a rate of 2°/min.

Analysis of TEM

A JEM-100SX transmission electron microscope (JEOL Co., Tokyo, Japan) was used to observe the dispersibility of the clay in the hybrids with an acceleration voltage of 120 kV. The sample was ultramicrotomed with a diamond knife on a Leica Ultracur UCT mic-
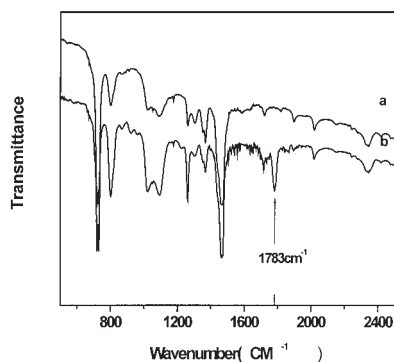
Figure 1 FTIR spectra of (a) HDPE and (b) PE-*g*-MAH–St.

rotome (Leica Co., Wetzlar, Germany) at room tem-perature to give a 70-nm-thick section.

Analysis of crystallization

DSC analyses were carried out with a TA Instrument 2920 modulated differential scanning calorimeter. The temperature and energy readings were calibrated with indium at each cooling rate employed in the measure-ments. All measurements were carried out in a nitro-gen atmosphere. The materials were heated from 30 to 150°C at a rate of 10°C/min to eliminate the heat history before cooling at 10°C/min.

TGA

TGA was employed to observe the thermal character of the composites on a TA Instrument Hi-Res TGA 2950 thermogravimetric analyzer under nitrogen at a scanning rate of 10°C/min from room temperature to 650°C.

Testing of the mechanical properties

The tensile test was carried out with a model LJ-1000 testing machine (Testing Machine Co., Guangzhou, China) at a crosshead speed of 10 mm/min and at room temperature, and the notched Izod type impact test was investigated with a model UJ-4 impact testing machine (Testing Machine Co., Chende, Hebei, China) at room temperature, according to GB1040-1996 and GB1843-1996, respectively.

RESULT AND DISCUSSION

Analysis of the grafters

As shown in Figure 1, on the curve of PE-*g*-MAH–St, a new peak appears at the wave number of 1783 cm^{-1} in comparison with that of the original PE; this is a characteristic vibration of the carbonyl group. This shows that MAH has successfully been grafted onto the backbone of PE. In most cases, the peak at the

wave number of 700 cm^{-1} is used to determine whether St has grafted onto the backbone. However, a peak for PE appears at the wave number of 700 cm^{-1}. Therefore, it is impossible to judge whether St has been grafted onto the backbone according to this peak. However, the new weak peaks appearing at the wave numbers of 1513 and 1600 cm^{-1}, which are also char-acteristic of the benzene ring, are used to prove that St has been grafted onto PE. Thus, we can conclude that MAH and St have been grafted, according to the free-radical reaction mechanism, onto the backbone of PE to form the MAH-*co*-St side chain.

Characterization of the PE-*g*-MAH–St/MMT nanocomposites

XRD analysis

In the XRD curve (Fig. 2) of organic MMT, there exists a (001) diffraction peak at 2.36°. According to the Bragg equation, $2d \sin \theta = n\lambda$, where n is the progres-sion of diffraction, the distance between interlayers (d) should be 3.74 nm. After mixing with PE-*g*-MAH–St, for PMST1 and PMST3 (as shown in Fig. 3), the (001) diffraction peaks shift from 2.360 for organic MMT to about 1.90 for the nanocomposites, and d increases from 3.74 to 4.65 nm; for PMST5, the (001) diffraction peak appears at the position of 2.18°, which corre-sponds to $d = 4.05$ nm. At the same time, all the intensities of the peak of MMT in the nanocomposites become much weaker than that of the original peak of pure organic MMT. This happens for the following two reasons: (1) the content of MMT is low in the composites, and (2) the molecular chains of PE are intercalated into MMT, and this results in the collapse of the orderly structure of MMT. The aforementioned results indicate that the molecular chains of PE have intercalated into MMT and formed PE-*g*-MAH–St nanocomposites. The grafting of the polar group onto
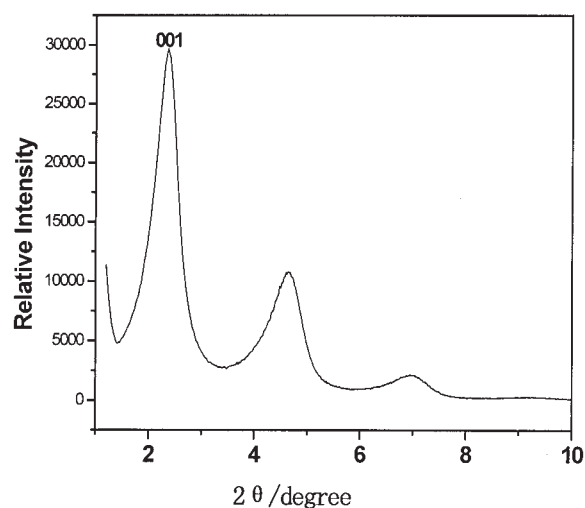
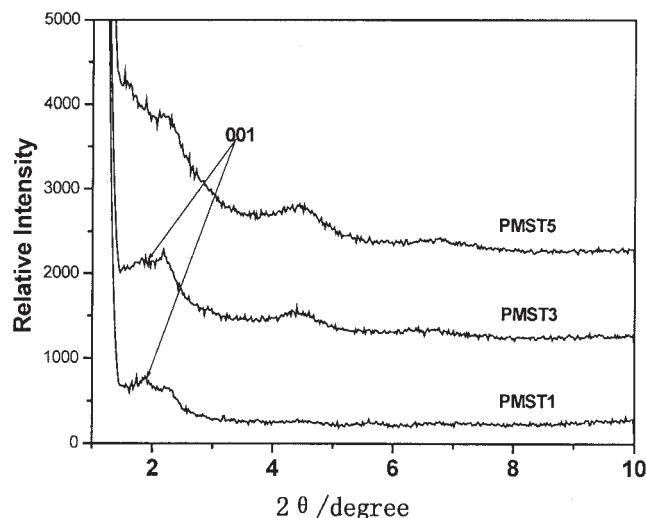

Figure 2 XRD pattern of organic MMT.

Figure 3 XRD patterns of PE-*g*-MAH–St/MMT nanocomposites.

Figure 4 TEM micrograph of a PE-*g*-MAH–St/MMT nanocomposite with 3 wt % MMT.

the backbone of PE can improve the hydrophilicity of PE. Therefore, the chain of the molecule of modified PE can enter the interlayers of MMT easily with the help of the interaction between the polar group and surface of MMT; this can increase the *d* value of MMT. This result is consistent with the results reported by Wang et al.[16]

TEM analysis

Most of the time, it is not enough to characterize the effect of the intercalation of polymer/clay nanocomposites just with XRD. TEM is also necessary to observe the dispersibility of MMT in the matrix. Thus, a TEM micrograph of PMST3 is shown in Figure 4. The dark lines in Figure 4 are the layers of MMT. It is easy to find that MMT has good dispersibility in the matrix. This also shows that PE-*g*-MAH–St has good compatibility with organic MMT. The TEM observation is in accordance with the results of XRD, and this further proves that nanocomposites have been obtained. On the basis of what has already been discussed, it is feasible to prepare PE/MMT nanocomposites via the grafting of PE with the functional polar monomer and then mixing with organic MMT.

Crystallization of the PE-*g*-MAH–St/MMT nanocomposites

The crystallization behavior of HDPE and PE-*g*-MAH–St/MMT has also been investigated with DSC, as shown in Figure 5. At first, in comparison with pristine PE, the temperature of the crystallization peak of PE-*g*-MAH–St increases about 2°, from 117 to 119°C. This means that the graft chain existing on the main chain of PE can act as a nucleating reagent to promote the heterogeneous nucleation of PE; this can increase
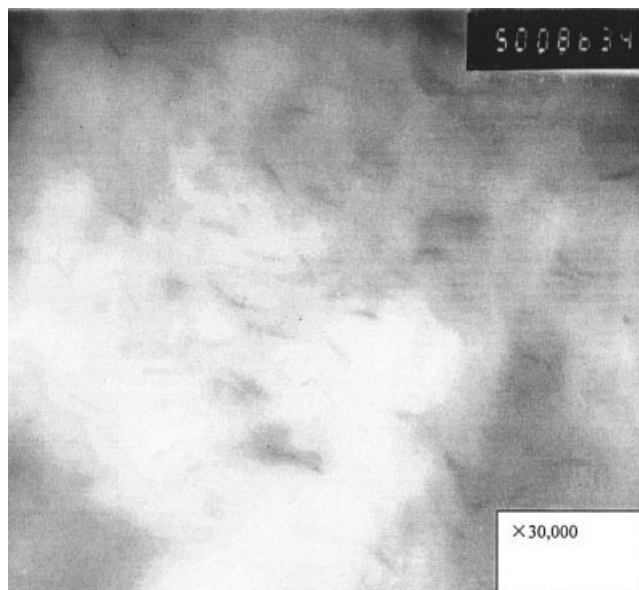
the crystallization rate and make the crystallization happen at a higher temperature. This result is consistent with that reported by Mai et al.[20] However, after PE-*g*-MAH–St is mixed with organic MMT, the difference in the crystallization temperature between PE-*g*-MAH–St and nanocomposites PMST1, PMST3, and PMST5 is slight. In general, the good dispersibility of MMT can promote the crystallization of the matrix; this has been proved in polypropylene.[21] This result may be due to the following two reasons. First, PE crystallizes at a very high crystallization rate because of its symmetry of structure; this may make it difficult to further improve the crystallization rate of PE. Second, graft chains on the main chain of PE act as nucleating reagents, so the addition of MMT does not improve the crystal speed further.

Thermal characteristics of the PE-*g*-MAH–St/MMT nanocomposites

In general, the thermal character of polymer/clay nanocomposites can be improved in comparison with
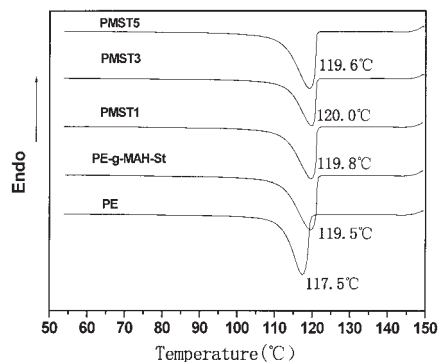

Figure 5 DSC curves of HDPE and PE-*g*-MAH–St/MMT nanocomposites.

that of the pristine matrix when the layers of MMT can be dispersed well in the matrix. Thus, in this study, TGA has been employed to investigate the thermal stability of the nanocomposites. Figure 6 presents the TGA curves of HDPE and PE-*g*-MAH–St/MMT nanocomposites. The decomposition temperature measured at the point of 20% mass loss (T_{20}) for HDPE is 442°C. However, for the nanocomposites, T_{20} is about 462°C, and the difference between PMST1, PMST3, and PMST5 is not significant. From the whole curve of TGA, the decomposition temperatures for the nanocomposites are always higher than that of HDPE. This shows that the thermal character is improved when the nanocomposites are obtained.

Mechanical properties of PE-*g*-MAH–St/organic MMT

The effects of the amount of organic MMT on the tensile strength and impact strength of PE-*g*-MAH–St are shown in Figure 7. The tensile strength increased first and then decreased; maximum values of the tensile strength (31.7 MPa) were achieved when the concentration of organic MMT was 3 wt %. However, in comparison with pure PE, the impact strength of the nanocomposites showed a slight decline.

CONCLUSIONS

Because of the lack of polar groups on the main chain of HDPE, it is difficult to prepare PE/MMT by direct melt mixing. Because of the difference in character between PE and inorganic MMT, two steps were taken: choosing organic MMT and modifying PE via grafting with MAH and St together. On the basis of these two steps, PE/MMT nanocomposites could be obtained by direct mixing. Because of the polar group on the backbone of the grafter of PE, it could improve the compatibility between MMT and PE, and the molecular chain of PE could insert into the interspace of MMT. At last, PE/MMT was obtained, as demonstrated by XRD and TEM. This point was in accor-
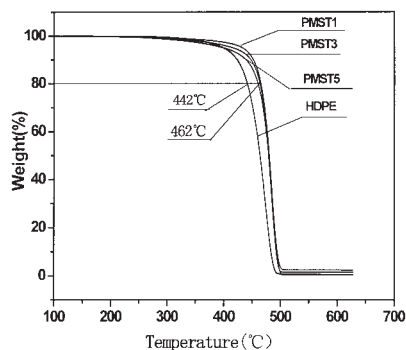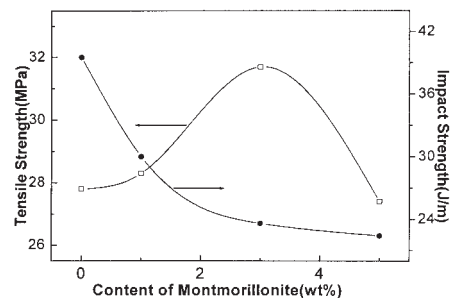

Figure 7   Plot of the tensile strength and impact strength of PE-*g*-MAH–St/MMT nanocomposites.

dance with the results reported by others concerning the nanocomposites of other polymers.[22] At the same time, the crystallization rate of PE improved when PE was grafted with MAH and St. However, the crystallization rate did not have a further improvement with the addition of organic MMT to PE-*g*-MAH–St. The thermal stability properties showed an obvious improvement in the TGA measurements, and the tensile strength of the nanocomposites reached the maximum value (31.7 MPa) when the loading of organic MMT was 3 wt %.

References

1. Messersimith, P. B.; Giannelis, E. P. J Polym Sci Part A: Polym Chem 1995, 33, 1047.
2. Bao, S. P.; Zhai, H. B.; Xu, W. B.; He, P. S. J Appl Polym Sci 2004, 92, 3822.
3. Kojima, Y.; Usuki, A.; Kawasumi, M.; Fukushima, Y.; Okada, A.; Kurauchi, T. J Mater Res 1993, 8, 1185.
4. Yano, K.; Usuki, A.; Okada, A.; Kurauchi, T.; Kamigato, O. J Polym Sci Part A: Polym Chem 1993, 31, 2493.
5. Giammelis, E. P. Adv Mater 1996, 8, 29.
6. Wang, Z.; Piammavaia, T. J. Chem Mater 1998, 10, 3769.
7. Xu, W. B.; Ge, M. L.; He, P. S. J Appl Polym Sci 2001, 82, 228.
8. Liang, G. D.; Xu, J. T.; Xu, W. B. J Appl Polym Sci 2004, 91, 3054.
9. Xu, W. B.; Bao, S. P.; He, P. S. J Appl Polym Sci 2002, 84, 842.
10. Hoai Nam, P.; Maiti, P.; Okamoto, M.; Kotaka, T.; Hasegawa, N.; Usuki, A. Polymer 2001, 42, 9633.
11. Alexandre, M.; Dubois, P.; Sun, T.; Garces, J. M.; Jerome, R. Polymer 2002, 42, 2123.
12. Shin, S. Y. A.; Simon, L. C.; Soares, J. B. P.; Scholz, G. Polymer 2003, 44, 5317.
13. Zhang, J. G.; Wilkie, C. A. Polym Degrad Stab 2003, 80, 163.
14. Kato, M.; Usuki, A.; Okada, A. J Appl Polym Sci 1997, 66, 1781.
15. Kawasumi, M.; Hasegawa, N.; Kato, M.; Usuki, A.; Okada, A. Macromolecules 1997, 30, 6333.
16. Wang, K. H.; Choi, M. H.; Koo, C. M.; Choi, Y. S.; Chung, I. J. Polymer 2001, 42, 9819.
17. Koo, C. M.; Ham, H. T.; Kim, S. O.; Wang, K. H.; Chung, I. J. Macromolecules 2002, 35, 5116.
18. Wang, K. H.; Chung, I. J.; Jang, M. C.; Keum, J. K.; Song, H. H. Macromolecules 2002, 35, 5529.
19. Gopakumar, T. O.; Lee, J. A.; Kontopoulou, M.; Parent, J. S. Polymer 2002, 43, 5483.
20. Mai, K. C.; Li, Z. J.; Zeng, H. M. Polym Mater Sci Eng (in Chinese) 2002, 18, 143.
21. Liu, X. H.; Wu, Q. J. Polymer 2001, 42, 10010.
22. Chen, T. K.; Tien, V. I.; Wei, K. H. Polymer 2000, 41, 1345.

Figure 6   TGA curves of PE-*g*-MAH–St/MMT nanocomposites.